A Computerized Method for Carrier Lifetime Measurement in PN Junctions at High and Low-Level Injection

Sebastián Montero, Ariel P. Cédola, Marcelo A. Cappelletti, and Eitel L. Peltzer y Blancá

***Abstract*— A system to determine the minority carrier lifetime in PN semiconductor junctions in the range of 50 ns to 100 µs has been developed. The measurement is performed by using the Open Circuit Voltage Decay (OCVD) technique. The equipment consists mainly of a data acquisition system based on a PIC16F877A microcontroller, connected to a computer, and software for the control of the entire system, data processing, storage and visualization of results.**

***Index Terms*—Carrier lifetime, experimental measurement, OCVD technique, microcontroller.**

I. Introduction

MINORITY carrier lifetime is a very important parameter in semiconductor science. Its knowledge allows to predict the electrical properties and to understand the physical processes involved on the semiconductor devices operation. Carrier lifetime depends on the nature of the semiconductor material, on the chemical processing during the device manufacturing, on the defects created by external mechanisms, for example radiation, among others. From an electrical viewpoint, carrier lifetime has a direct influence on many device parameters, like the reverse current, the carrier densities and the reverse recovery time in diodes, the current gain in bipolar transistors and the conversion efficiency in solar cells, for example. On the other hand, it allows to obtain information about defects in semiconductors and, as a consequence, to gain insight into their quality. For all these reasons, carrier lifetime measurement is of great relevance in device research.

Two fundamental processes that take place in a semiconductor are hole and electron recombination and generation. The generation creates carriers, whereas the recombination annihilates them. Lifetime of minority carriers is the mean time elapsed until a carrier disappears by recombination. Depending on the way the energy is released during this process, the recombination is classified into Shockley-Read-Hall recombination, radiative band-to-band recombination and Auger recombination [1], [2]. The influence of each of these mechanisms on the carrier lifetime τ_r can be expressed by

$$\frac{1}{\tau_r} = \frac{1}{\tau_{SRH}} + \frac{1}{\tau_{RAD}} + \frac{1}{\tau_A}, \quad (1)$$

where τ_{SRH}, τ_{RAD} and τ_A are the carrier lifetimes related to the three processes cited above. Another parameter that has a direct influence on the carrier lifetime obtained from a measurement is the surface recombination rate. Actually, the measured lifetime is an effective lifetime that includes both, surface and bulk components. It can be written as [3]

$$\tau_{eff} = \left(\frac{1}{\tau_r} + \frac{1}{\tau_s} \right)^{-1}, \quad (2)$$

where τ_r and τ_s are the lifetimes associated with bulk recombination and surface recombination, respectively.

A number of methods have been developed in order to determine the minority carrier lifetime on semiconductor wafers and devices. Photoconductance decay (PCD) and its variants [4], [5], Quasi Steady State Photoconductance (QSSPC) [6] and Free Carrier Absorption (FCA) [7] are the most common methods applied to lifetime measurement on wafers, whereas Reverse Recovery (RR) [8] and Open Circuit Voltage Decay (OCVD) [9] are the most used in experiments on PN junctions. OCVD presents a few advantages over RR method. Furthermore, it has been shown through experimental and simulation results that OCVD is more exact than RR [10].

In this work, the implementation of a system to measure the carrier lifetime by using the OCVD technique is reported. The system, which works attached to a computer, includes

S. Montero is with the Grupo de Estudio de Materiales y Dispositivos Electrónicos (GEMyDE), Departamento de Electrotecnia, Facultad de Ingeniería, Universidad Nacional de La Plata, 48 y 116, CC.91, La Plata (1900), Argentina (e-mail: seba.montero@ing.unlp.edu.ar).

A. P. Cédola is with the Grupo de Estudio de Materiales y Dispositivos Electrónicos (GEMyDE), Departamento de Electrotecnia, Facultad de Ingeniería, Universidad Nacional de La Plata, 48 y 116, CC.91, La Plata (1900), Argentina (Phone +54 0221 4236690, Fax +54 0221 4236690, e-mail: ariel.cedola@ing.unlp.edu.ar).

M. A. Cappelletti is with the Grupo de Estudio de Materiales y Dispositivos Electrónicos (GEMyDE), Departamento de Electrotecnia, Facultad de Ingeniería, Universidad Nacional de La Plata, 48 y 116, CC.91, La Plata (1900), Argentina. He also is with the Instituto de Física de Líquidos y Sistemas Biológicos (IFLYSIB), CONICET-UNLP-CIC, La Plata, Argentina (e-mail: marcelo.cappelletti@ing.unlp.edu.ar).

E. L. Peltzer y Blancá is with the Grupo de Estudio de Materiales y Dispositivos Electrónicos (GEMyDE), Departamento de Electrotecnia, Facultad de Ingeniería, Universidad Nacional de La Plata, 48 y 116, CC.91, La Plata (1900), Argentina. He also is with the Instituto de Física de Líquidos y Sistemas Biológicos (IFLYSIB), CONICET-UNLP-CIC, La Plata, Argentina (e-mail: eitelpyb@ing.unlp.edu.ar).

software and hardware developments. In Section II, an overview of the OCVD method is presented. In Section III the design and implementation of the system hardware is explained in detail. Section IV covers the software development and Section V summarizes the results of experimental carrier lifetime measurements performed over different PN devices.

II. Fundamentals of the OCVD Method

The OCVD is a simple and non-destructive technique for the determination of minority carrier lifetime in semiconductor diodes. It consists in applying a current pulse to the device under test (DUT), in order to forward biasing the junction, and then to observe the voltage decay at the junction in an open circuit condition. This decay is linear and it is product of the recombination of the excess carriers injected to the DUT by the current pulse.

At a low-level injection condition, the effective lifetime can be calculated by the expression [9]

$$\tau_{eff(ll)} = -\frac{kT}{q}\left(\frac{dV(t)}{dt}\right)^{-1}, \qquad (3)$$

where $V(t)$ is the diode voltage, k is the Boltzman constant, q is the electron charge and T is the temperature. The slope of the linear diode voltage decay is inversely proportional to $\tau_{eff(ll)}$.

Fig. 1 shows the voltage decay as a function of time. Once expired the initial voltage drop, due to the serial resistance the device, the junction voltage decreases linearly (ideal response). From this linear decay the effective lifetime is determined. The picture also shows some non-ideal effects over the response of the diode to the current pulse. The junction capacitance reduces the voltage decay slope, leading to an overestimation of the lifetime. On the contrary, the carrier recombination in the depletion region and the diode shunt resistance produce a lifetime underestimation [11]. Another effect present in the initial portion of the voltage decay is a non-linearity due to the recombination of carriers in the device emitter. Excess carriers in this region recombine faster than excess carriers in the base, inducing a flux of carriers from base to emitter and a more pronounced decay at the beginning of the curve [12].

At a high-level injection condition, and assuming a uniform density of carriers in the base region, the lifetime can be calculated by [13]

$$\tau_{eff(hl)} = -2\frac{kT}{q}\left(\frac{dV(t)}{dt}\right)^{-1}. \qquad (4)$$

In this situation two linear slopes are obtained, as can be seen in Fig. 2. The first of them ($t_1<t<t_2$) is related to the recombination of excess carriers in the quasi-neutral regions at a high-level injection condition. The second one ($t_2<t<t_3$), depending on the initial voltage, can be attributed to the recombination in the depletion region or to the recombination in the quasi-neutral regions when the level of injection is low [13].

III. Development of the Measurement System

The block diagram of the system developed for the measurement of the minority carrier lifetime on PN junctions is shown in Fig. 3. The Excitation stage biases the device

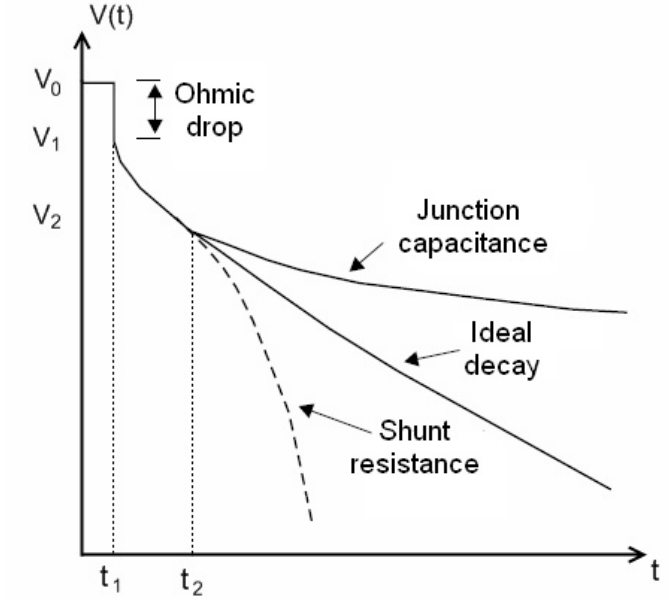

Fig. 1. Theoretical curve showing the open circuit voltage decay of a diode at a low-level injection condition. Non-ideal effects are shown too [11].

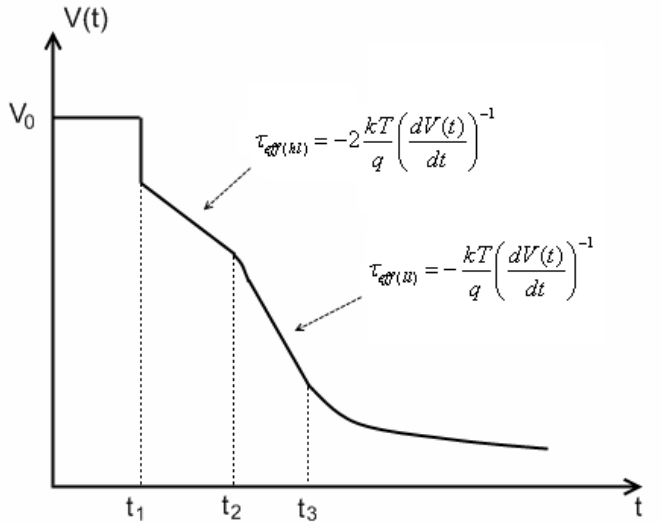

Fig. 2. Theoretical curve of the voltage decay for a diode at a high-level injection condition.

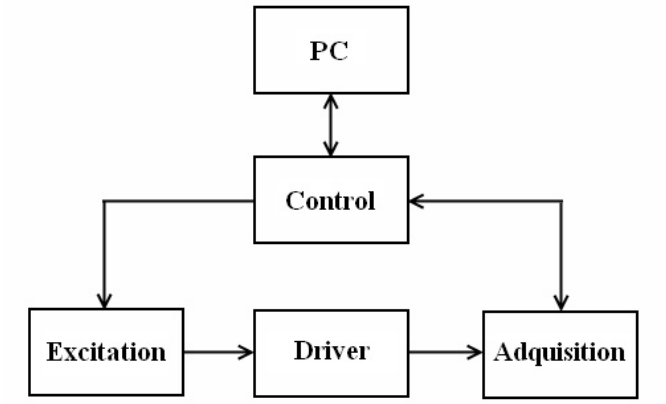

Fig. 3. Block diagram of the developed carrier lifetime measurement system.

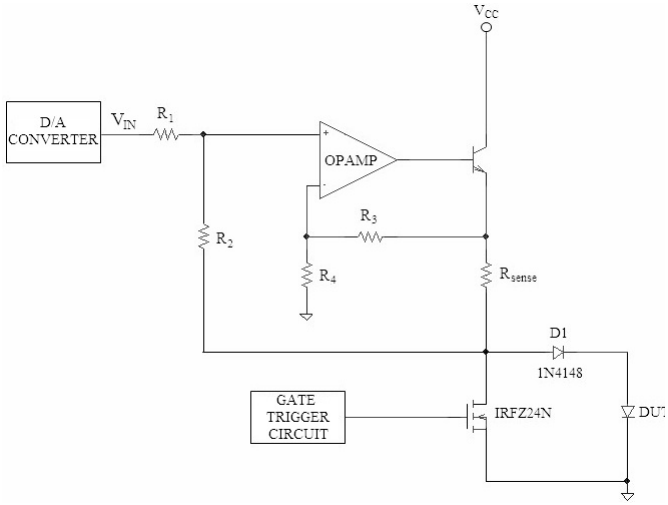

Fig. 5. Scheme of the Excitation stage with details of the electronic circuit.

under analysis and generates the open circuit condition required by the OCVD method. The Acquisition stage digitizes the diode voltage decay by taking samples at a very high rate and saves these samples for their subsequent transfer to the computer. The Driver stage adapts the signal entering to the Acquisition stage. Finally, the Control stage works as an interface between the Computer (PC) and the rest of the system. Through the computer software the measurement parameters are configured, the curves are obtained and the carrier lifetime is calculated.

A. Excitation Stage

Fig. 4 shows the basic circuit of the Excitation stage. The current source applies a forward bias to the DUT. The switch and the D1 diode establish the open circuit condition that gives place to the voltage decay. The current source was implemented by using a voltage-current converter. By applying a voltage in the range of 0.1 V to 1.5 V, selected from the Control stage through a D/A converter, the source supplies to the DUT a regulated current from 0 to 150 mA. A more detailed scheme of the circuit is shown in Fig. 5. The operational amplifier along with R_1, R_2, R_3, R_4 and R_{SENSE} resistors make up the voltage-current converter, whose output current is given by the relation V_{IN}/R_{SENSE}. The switch consists of a high speed IRFZ24N MOSFET transistor, with a low input capacitance (<500 pF) and a low on- resistance (<0.07 Ω). The low input capacitance gives the device a switching speed that has no influence on the voltage decay to be observed. The low on-resistance makes negligible the voltage drop through the switch.

An important issue considered was the leakage current of the D1 diode. This current must be small enough in order to prevent the charge accumulated in the DUT flow through the switch when it becomes closed. For this reason an 1N4148 diode was used. Besides a low leakage current (<1μA), this diode has a very short reverse recovery time (t_{rr}≈4 ns), which assures the no alteration of the voltage decay slope to be measured.

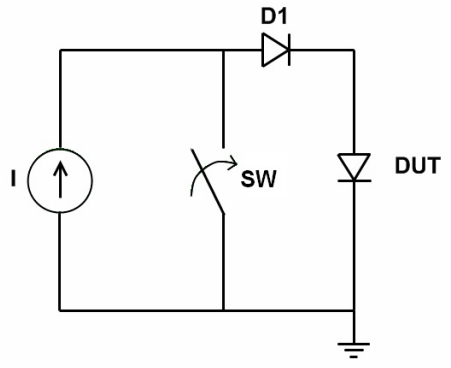

Fig. 4. Simplified scheme of the Excitation stage.

B. Acquisition Stage

The aim of this stage is to read a transient phenomenon, that means, a non-repetitive signal having place during a very short time. This signal is the decay of the open circuit junction voltage. The Acquisition stage digitizes the analog input signal and saves the taken samples. Once these steps are finished, the Control stage transfers the data to the Computer for their processing.

An A/D converter and a parallel FIFO memory were used for the implementation of this stage, in the configuration pictured in Fig. 6. The speed of the system mainly depends on the conversion time (T_C), imposed by the A/D converter. The lower limit of the system measurement range is fixed by the T_C and the acceptable error in the measurement of the voltage decay slope. The upper limit is defined by the memory capacity.

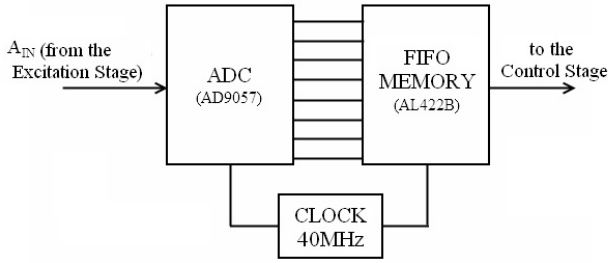

Fig. 6. Block diagram of the Acquisition stage.

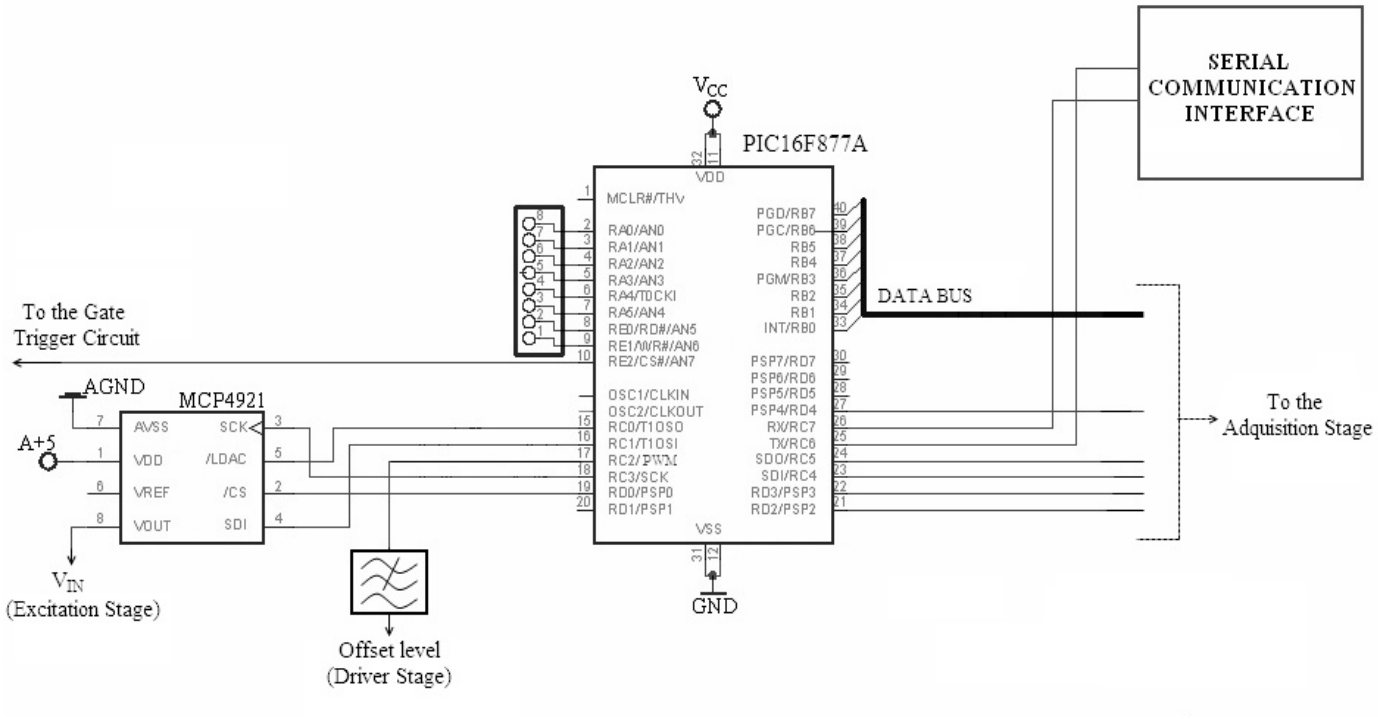

Fig. 7. Schematic diagram of the Control stage.

The A/D converter used in the system was an AD9057 [14]. This device has an 8 bit resolution and a maximum conversion rate of 40 MSPS, equivalent to a conversion time of 25 ns. In this way, the lower limit of the measurement range, considering an instrumental error of 10%, was established in 50 ns. The upper limit, for practical sense, was fixed in 100 µs. The memory selected was an AL422B [15], with a capacity of 384 KB and an operation frequency of 50 MHz. This memory is organized in an FIFO configuration. When the memory is read, the data are extracted in the same order that were written. Being not necessary the use of a more complex system to read and write data to memory, the design of this stage was greatly simplified.

C. *Driver Stage*

This stage carries out the conditioning of the transient signal coming from the Excitation stage, adjusting it to the input range of the A/D converter, from 2 V to 3 V. This stage, therefore, shifts in 2 V the DUT voltage decay and limits its excursion to 1 V.

The Driver stage was designed so that its input impedance be much greater than that of the device under analysis, in order to turn negligible the insertion error.

It is possible to select, through an array of jumpers on the printed circuit board, the voltage range at the A/D converter input: 0.5 V, 0.7 V and 2 V. This setting, along with the adjustment of the shift level, allows to fit the curve portion of interest to the input range of the A/D converter and then to minimize the errors in the slope measurement.

D. *Control Stage*

The main component of this stage is a microcontroller, as can be seen in Fig. 7. This device regulates the current applied to the DUT by means of a D/A converter, commands the start of the measurement, manages the transfer of data from FIFO memory to the computer through a serial communication interface and signalizes the system state. A PIC16F877A [16] 8 bit microcontroller was used, since it meets all necessary requirements to control the different system stages. The following are some of its main features:

1) 35 instructions RISC CPU.
2) Maximum operation frequency of 20 MHz (200 ns instruction cycle).
3) USART module.
4) Master synchronous serial port module, to be operated as SPI or I^2C.
5) Two capture/compare/PWM modules.
6) 5 parallel ports (A, B, C, D, E) with input/output independent programmable lines.

The shift level of the voltage decay in the Driver stage is adjusted by the PWM module and a low-pass filter. The USART module is connected to the serial communication interface, whose main component is a MAX232 [17] driver/receiver integrated circuit, that converts the microcontroller TTL/CMOS digital signals to RS232 levels as required by the computer to establish the communication. Through the SPI module the microcontroller communicates with the MCP4921 [18] D/A converter, that defines the input voltage to the current source to forward bias the DUT.

Fig. 8 shows a photograph of the developed system.

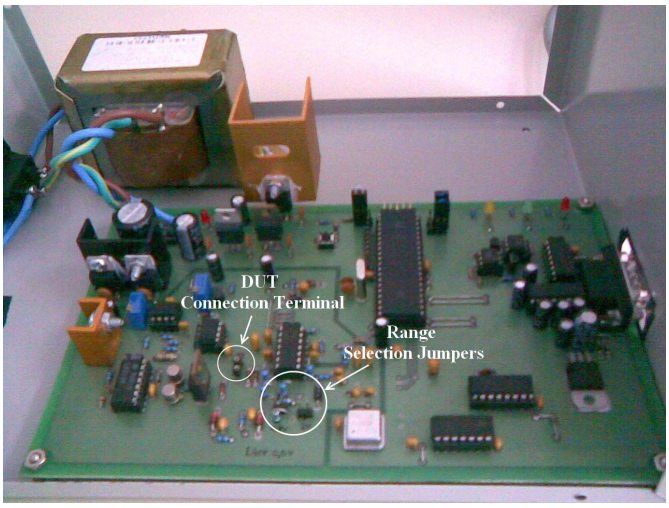

Fig. 8. Internal view of the developed system. The range selection jumpers and the DUT connection terminals are emphasized.

IV. Measurement Software

A software application in Visual Basic 6.0 environment was developed to configure the system parameters, visualize the measurements results and calculate the carrier lifetime through a computer. In Fig. 9 a capture of the main screen of the application can be observed. The dropdown list named Port allows to choose the serial port to which the instrument is connected. The Current slider control is used to set the biasing current to be applied to the DUT. Through the Range Selection menu the input range of the instrument can be selected. This value must be configured according to the state of the range selection jumpers on the printed circuit. The Time Base list allows to define the number of samples to be plotted.

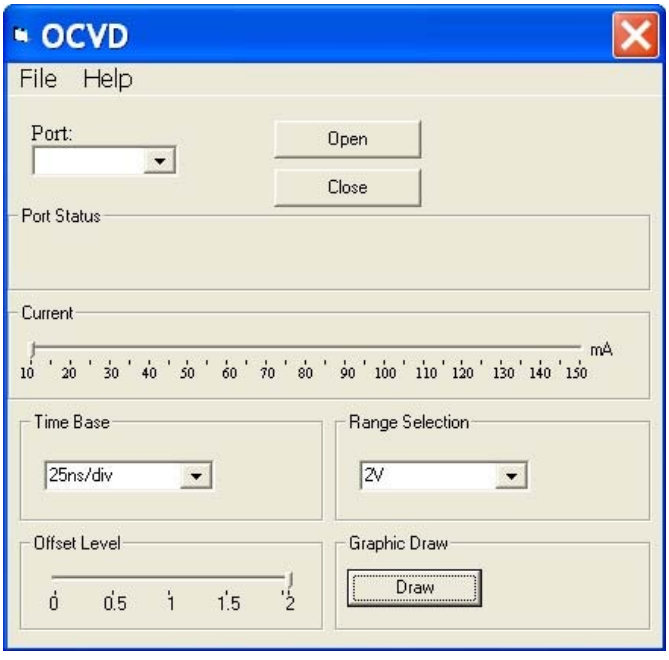

Fig. 9. Main screen of the software for the control of the measurement

By means of the Offset Level control, the signal is fitted into the visualization area. Finally, the Draw button starts the measurement.

The more recommendable way to take a measurement is, once connected the instrument to the correct serial port, to put the range jumper in the 2 V position, configure the current according to the device to be studied and leave the shift control in 2 V. After the examination of the obtained curve, the appropriate shift level and range can be determined for a more accurate subsequent measurement.

Fig. 10 shows a capture of the window where the DUT voltage decay is visualized. There are three buttons in the upper part of the screen: Reset, Filter and Fit. With the Filter button, the samples are processed by a digital 10 MHz low-pass filter that smoothes the fast variations of the signal provoked by noise. The Fit button applies the least squares method with a 6^{th} order polynomial (red curve) to the taken samples (black curve). Finally, the Reset button returns the plot to its original form.

A pair of cursors is used to calculate the carrier lifetime from the visualized curve. These cursors must be positioned on the two points of the curve that agree with the extremes of the linear slope. By using the Lifetime (hl) or Lifetime (ll) buttons, the high or low-level injection condition carrier lifetime is determined, respectively. These commands order the software to calculate the carrier lifetimes by solving (3) and (4).

V. Experimental Results

A number of experimental measurements were made over commercial diodes. The obtained curves were contrasted with an oscilloscope HP4603B, with an error below 8% in the determination of the slopes. The difference between both methods stayed less than 2% in all cases. On the other hand,

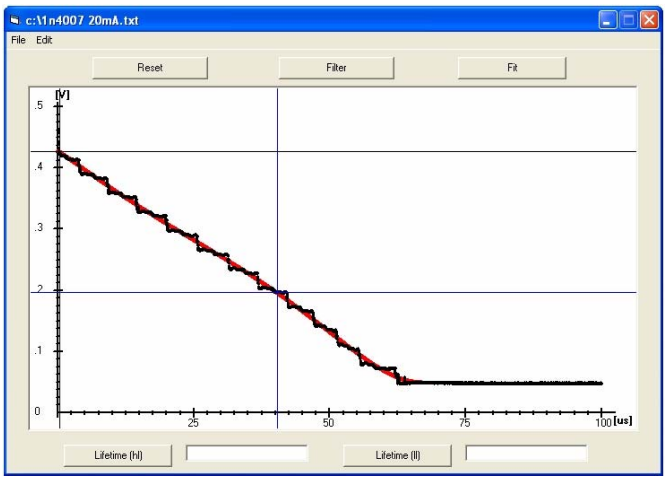

Fig. 10. Window where the open circuit voltage decay curve is visualized. At the lower part of the screen the buttons used to calculate the carrier lifetimes can be observed.

it was concluded that the obtained results are in good agreement with data published in the literature.

Table I summarizes the experimental lifetimes measured with the developed system. Although the semiconductor materials that compose the analyzed devices are known, there is not available information about doping densities and other relevant parameters. This fact explains the differences between the carriers lifetimes obtained for devices based on the same material.

Fig. 11 shows three of the experimental curves visualized with the system.

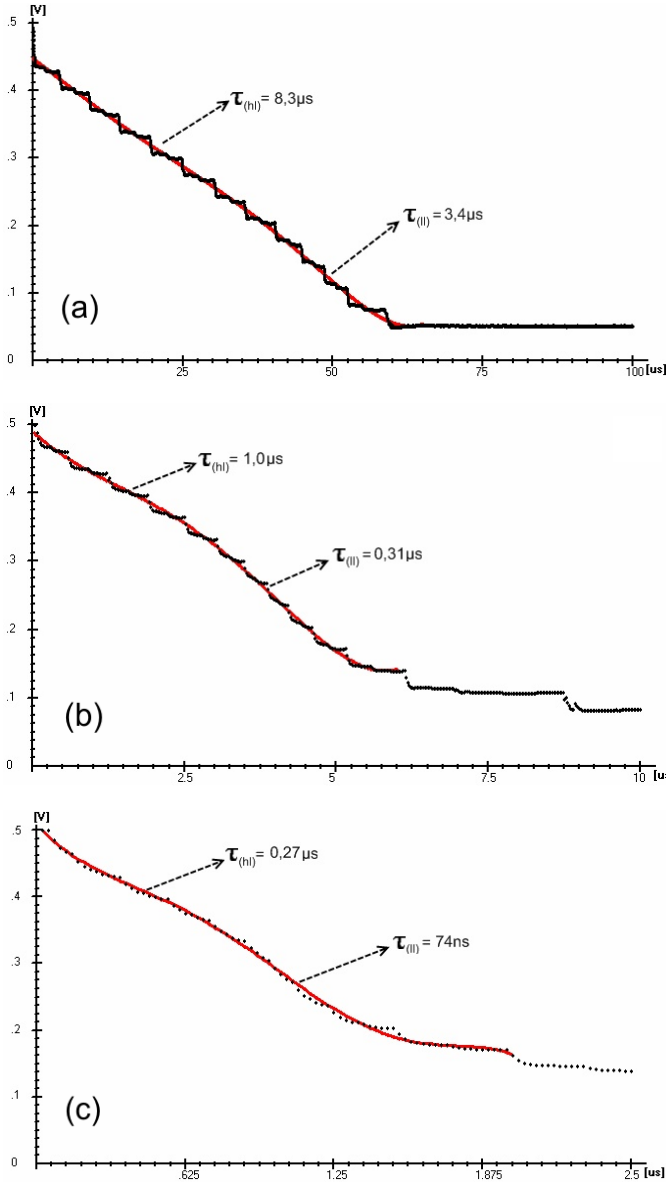

Fig. 11. Voltage decay curves obtained for (a) a silicon rectifier diode model 1N5408; (b) an infrared LED model IR333; (c) a red LED model L53EC. In all cases a biasing current of 20 mA was applied. The black curves correspond to the sampled data whereas the red curves represent the numerical fit made by the software to each measurement.

TABLE I
LIFETIME MEASUREMENTS CARRIED OUT OVER COMMERCIAL DIODES

DUT	Semiconductor	Lifetime $\tau_{(hl)}$	Lifetime $\tau_{(ll)}$
1N4007(1)	Si	10,0µs	4,0µs
1N4007(2)		8,3µs	3,4µs
1N4007(3)		8,9µs	4,0µs
1N4007(4)		8,9µs	3,8µs
1N5408(1)		22µs	8,3µs
1N5408(2)		15µs	7,0µs
6A10	Si	38µs	15µs
WP7113F3BT	GaAs	0,92µs	0,20µs
IR333	GaAlAs	1,0µs	0,31µs
4N25	GaAs	1,6µs	0,34µs
4N25(2)		1,9µs	0,50µs
L53EC	GaAsP/GaP	0,27µs	74ns

VI. CONCLUSION

An instrument able to measure the minority carrier lifetime in semiconductor diodes has been designed and implemented, with highly satisfactory results. The system is based on the OCVD technique. The range of the instrument covers five orders of magnitude, from 50 ns to 100 µs. The design was divided into four main stages: Excitation, Acquisition, Driver and Control. A careful analysis of these stages was carried out, the appropriate electronic devices were selected and the circuit layouts were designed. Software for the control of the system, data processing and visualization of results was developed too. The obtained measurements agree well with previous results published in the literature. In spite of the equipment was conceived to measure the minority carrier lifetime in diodes, it is feasible its application to experiments on semiconductor wafers.

REFERENCES

[1] J. P. McKelvey, *Solid State and Semiconductor Physics*. Krieger Pub Co, 1982, ch. 10.
[2] S. S. Li, *Semiconductor Physical Electronics.* Plenum Press, 1993, ch. 6.
[3] D. K. Schroder, "Carrier lifetimes in silicon," *IEEE Trans. Electron Devices*, vol. ED-44, pp. 160-170, Jan. 1997.
[4] "IRE Standards on Solid-State Devices: Measurement of minority-carrier lifetime in germanium and silicon by the method of photoconductive decay", *IRE Standards on Solid-State Devices*, vol. 49, pp. 1292-1299, 1961.
[5] F. P. Giles and R. J. Schwartz, "Computational separation of bulk and surface recombination using contactless photoconductive decay," School of Electrical and Computer Engineering, Purdue University, IN, Tech. Rep. TR-ECE 96-6, 1996.
[6] R. Sinton and A. Cuevas, "Contactless determination of current–voltage characteristics and minority carrier lifetimes in semiconductors from quasi-steady-state photoconductance data," *Appl. Phys. Lett.*, vol. 69, pp. 2510-2512, Oct. 1996.
[7] F. P. Giles, F. Sanii, R. J. Schwartz, and J. L. Gray, "Nondestructive contactless measurement of Bulk lifetime and Surface recombination using single pass infrared free carrier absorption," in *Conf. Rec. 1991 IEEE Photovoltaic Specialist Conference*, vol. 1, pp. 223-228.
[8] H. J. Kuno, "Analysis and characterization of P-N junction diode switching," *IEEE Trans. Electron Devices*, vol. ED-11, pp. 8-14, Jan. 1964.
[9] S.R. Lederhandler and L.J. Giacoletto, "Measurement of minority carrier lifetime and surface effects in junction devices," *Proc. IRE*, vol. 43, pp. 477–483, Apr. 1955.
[10] M. Derdouri, P. Leturcq, and A. Muroz-Yague, "A comparative study of methods of measuring carrier lifetime in p-i-n devices," *IEEE Trans. Electron Devices*, vol. ED-27, pp. 2097-2101, Nov. 1980.

[11] R. Salach-Bielecki, T. Pisarkiewicz, T. Staiñski, and P. Wójcik, "Influence of junction parameters on the open circuit voltage decay in solar cells," *Opto-Electron. Rev.*, vol. 12, pp. 79-83, Jan. 2004.
[12] U. C. Ray, S. K. Arwal, and S. C. Jain, "Theory and experiments on open circuit voltage decay of p-n junctions diodes with arbitrary base width, including the effects of built-in drift field in the base and recombinations in the emitter," *J. Appl. Phys.*, vol. 53, pp. 9122-9129, Dec. 1982.
[13] H. G. Bhimnathwala, S. D. Tyagi, S. Bothra, S. K. Ghandhi, and J. M. Borrego, "Lifetime measurements by open circuit voltage decay in GaAs and InP diodes," in *Conf. Rec. 1990 IEEE Photovoltaic Specialist Conference*, vol. 1, pp. 394–398.
[14] *Analog Devices AD9057 8-Bit 40MSPS/60MSPS/80MSPS A/D Converter Datasheet*, Analog Devices Inc., Wilmington, MA, 2003.
[15] *Averlogic AL422B Memory Datasheet*, Averlogic Technologies Inc., Taiwan, 2001.
[16] *Microchip PIC16F87XA 28/40/44-Pin Enhanced Flash Microcontroller Datasheet*, Microchip Technology Inc., Chandler, AZ, 2003.
[17] *Maxim MAX232 Driver/Receiver Datasheet*, Maxim Integrated Products Inc., Sunnyvale, CA, 2001.
[18] *Microchip MCP4921/4922 12-Bit D/A Converter Datasheet*, Microchip Technology Inc., Chandler, AZ, 2007.